FERMILAB-Proposal-0670

THE ROCKEFELLER UNIVERSITY
1230 YORK AVENUE · NEW YORK, NEW YORK 10021

January 14, 1981

Dr. Norman Gelfand
Program Planning Office MS #105
Fermilab
P.O. Box 500
Batavia, IL 60510

Dear Norman,

This letter of intent is being written in response to the Fermilab call for proposals for use of the tagged photon facility when 1000 GeV protons become available from the Energy Double/Saver. The schedule of our experiment E-612 in the tagged photon beam is such that it seems to us premature to present a new, detailed proposal prior to the February 1, 1981 deadline. However, since we now have a working detector and expect to succeed in making the measurements approved in E-612, a general program of new physics for the future can be outlined at this time and is the subject of this letter of intent. The specifics of a future proposal will, of course, depend on the results of E-612.

The present status of E-612 is as follows: As of this date, our detector, TREAD (The Recoil Energy and Angle Detector), has been completed and tested. It is now being installed in the Tagged Photon Laboratory (TPL). During the past several months, TREAD has been subjected to an extensive series of performance and safety tests, the latter under the supervision of the appropriate Fermilab safety committees. Under established operating rules and conditions, TREAD has now been approved for installation and operation in the TPL.

Performance tests, using cosmic rays and radioactive sources, have shown that TREAD works well with pure hydrogen as the drift gas. Thus the necessity of separating the hydrogen target from the drift gas with an intervening thin mylar wall has been eliminated. This will reduce multiple scattering and greatly simplify operation. The tests have been carried out at pressures up to 15 atm with an overall drift potential up to the maximum available of 200 KV (the original proposal called for 10 atm; the vessel has been tested and approved for use to 20 atm). Cosmic ray tracks crossing TREAD at varying distances along the chamber axis have been used to simulate recoiling protons. Reconstruction of these tracks provides data for analysis of distortion, resolution and stability of the device. The results of the tests are very gratifying. Two figures are attached. One displays a scatter plot of the deviation on a single wire of the measured from the fitted point as a function of drift distance, the

43 pgs.

other is the projection on the abscissa of the scatter plot. The measured r.m.s. deviation averaged over the length of the chamber is $\sigma \approx 400$ μm. This value is already somewhat smaller than the estimate used in our proposal. No serious distortions due to inhomogeneities in the electric field or other sources are observed at this level of accuracy. The scatter plot indicates that the resolution is approximately proportional to $L^{\frac{1}{2}}$ as expected from diffusion of the electrons in the gas. Full tests of long term stability due to temperature variation will have to await installation in TPL and activation of the solenoidal magnet.

In E-612, we expect to measure the diffractive dissociation of photons for $0.01 < |t| < 0.1$ (GeV/c)^2 and $M_X{}^2/s \lesssim 0.1$ covering the mass range $M_X \lesssim 5$ GeV for the presently available tagged photon energies (20-140 GeV). Specifically, we will measure $d^2\sigma/dtdM_X{}^2$ with resolutions $\Delta t = 0.002$ (GeV/c)^2 and $\Delta M_X / M_X \lesssim 1.5\%$. Our sensitivity is such that in the scheduled run we expect $\approx$ 30 events per nanobarn cross section. We expect to observe, with excellent resolution, the known vector mesons in our mass range and to study the behavior of the continuum. We also hope to see new resonances, some of which have been tentatively identified in e^+e^- experiments.

It seems to us clear that there are two general directions, not mutually exclusive, in which we will wish to pursue further this line of research: (1) to increase the mass range and the sensitivity of the experiment, and (2) to use TREAD as a trigger for the TPL multiparticle spectrometer facility to study final states with the quantum numbers of the photon which are labeled in mass.

A routine upgrading of the tagged photon beam will increase our available diffractive mass range to $\lesssim$ 7 GeV. Greater intensity, especially for the highest energy photons, would improve the experiment substantially. One of our collaborators (MJT) has made a detailed analysis of the enhancement in the photon spectrum which can be achieved by the use of coherent brehmstrahlung from a diamond crystal. The attached paper, which was delivered at a recent symposium in Lausanne, discusses these considerations. A great improvement in the tagged photon beam using this technique appears eminently feasible and we urge that it be made an integral part of the plan for upgrading the energy of the tagged photon beam. Our group is prepared to take an active role in a collaboration to achieve this end.

It has long been obvious that TREAD can provide a trigger for the TPL Spectrometer Facility to study final states. Such a trigger would not only label the mass of each event, but would assure the diffractive origin of the event and thus that the final state carries the quantum numbers of the photon. Such a study would become especially important if we are able to identify new resonances in E-612. The manpower in our present collaboration is not adequate

to operate TREAD and the TPL Spectrometer Facility simultaneously. Some tentative discussions with physicists now using the TPL Spectrometer suggest that it should be possible to interest enough new collaborators to carry out this project successfully.

To summarize briefly -- when results from TREAD become available, we expect to propose a new program using an upgraded tagged photon beam. This program will include some or all of the following: increased mass range, increased sensitivity by improving the beam with coherent brehmstrahlung from a diamond crystal, and use of the TPL Spectrometer Facility in conjunction with TREAD to study final states.

Sincerely,

K. Goulianos

K. Goulianos
Spokesman for E-612

Enclosure

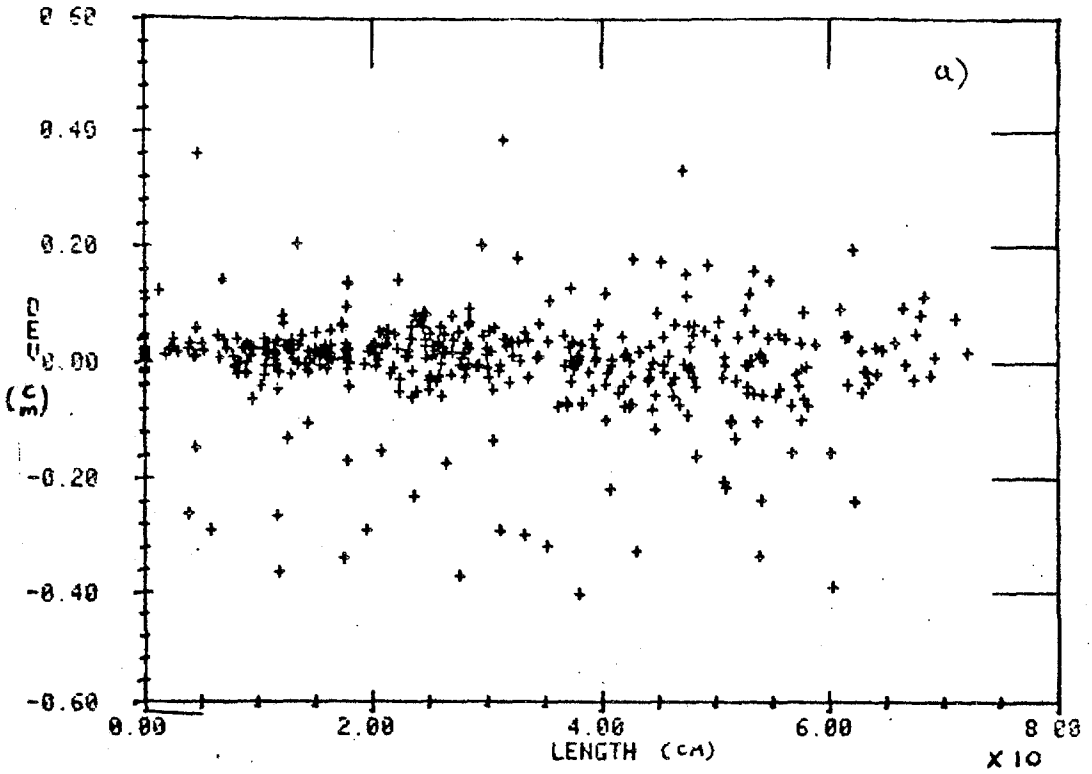

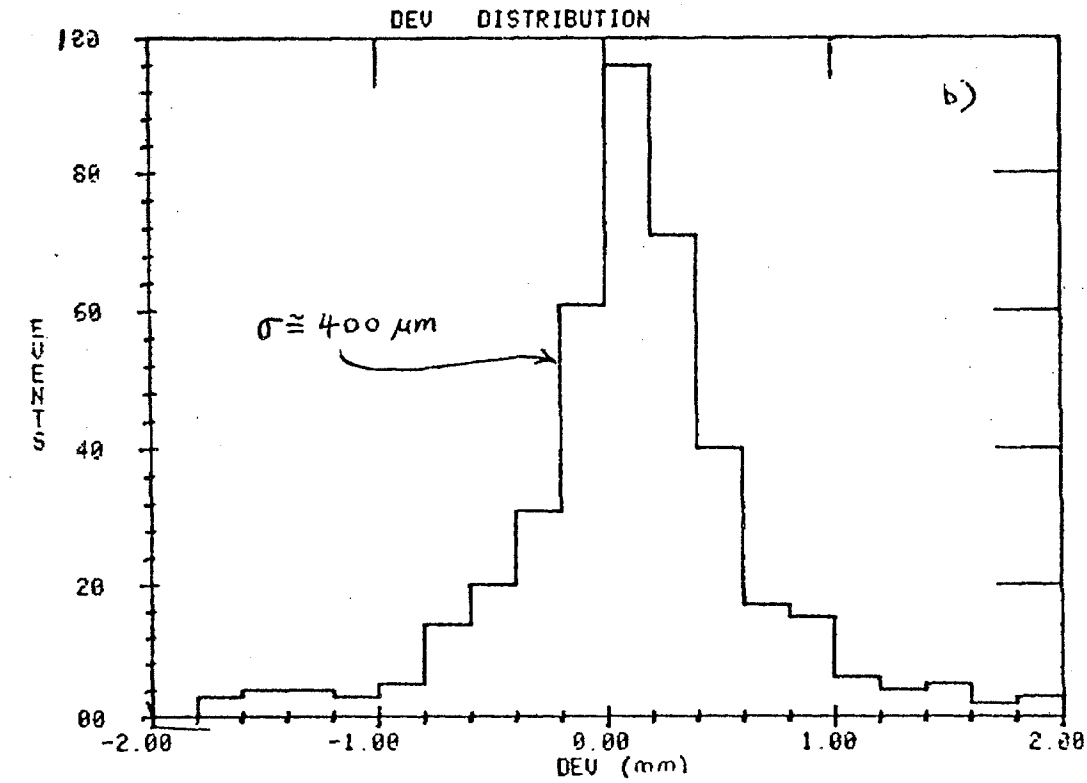

Position Resolution in TREAD in H_2 gas at 15 Atmospheres

a) plotted against drift length
b) projected.

1980 Symposium on High Energy Physics with Polarized Beams and Polarized Targets
9/25/80 - 10/1/80 Lausanne, Switzerland

BNL-28586

FEATURES OF POSSIBLE POLARIZED PHOTON BEAMS AT HIGH ENERGY AND CORRESPONDING PHYSICS PROGRAMME or THE PROTON STRUCTURE FUNCTION USING REAL PHOTONS*

Michael J. Tannenbaum
Accelerator Department, ISABELLE Project
Brookhaven National Laboratory
Upton, New York 11973

ABSTRACT

In the range of electron energies available at Fermilab, 100 GeV $\leq$ E $\leq$ 500 GeV, coherent Bremsstrahlung in crystals, particularly diamond, gives a huge enhancement to the equivalent photon spectrum at large values of x where x = k/E. The photons in this enhancement are polarized. Requirements on electron beam energy spread, angular divergence and spot size imposed by the use of a diamond as a radiator are discussed. The physics program emphasizes hard processes and tests of QCD using polarization.

INTRODUCTION

Consider an incident electron of energy E which radiates a photon of energy k in the field of a nucleus leaving a residual electron of energy E-k.

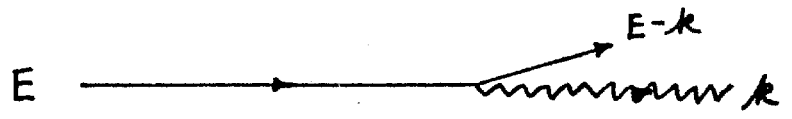

Fig. 1

For an ordinary amorphous radiator the photon yield per incident electron is

$$dN = t \times dk/k \times F(x)$$

where t is the radiator thickness in radiation lengths and x=k/E. For thin radiators,

$$F(x) = [1 + (1-x)^2 - 2/3\ (1-x)] \tilde{=} 1.$$

It is also a customary to write these expressions as

$$k\ dN/dk = t \times F(x)$$

The quantity k(dN/dk) is called the spectrum of "equivalent photons".

The actual number of photons produced at high energies is proportional to 1/k and thus decreases with increasing photon energy. In order to get more photons, the radiator thickness can be increased. However, for radiator thicknesses $\geq$ 0.10, the high energy photon yield is decreased because the infra-red divergent low energy photon tail causes the energy of the incident electron beam to degrade as it passes through the radiator.[1] Furthermore, multi-photon emission increases; and loss

* Work performed under the auspices of the U.S. Department of Energy

of photons via conversion in the radiator becomes significant.

How can the yield of high energy photons be increased?

In the Fermilab-Tevatron energy range of $100 \leq E \leq 500$ GeV, coherent Bremsstrahlung in crystals, particularly diamond, can be used to obtain a huge enhancement of the equivalent photon spectrum at large x.

PRINCIPLES OF COHERENT BREMSSTRAHLUNG

The principles and practices of coherent Bremsstrahlung in crystals are very clearly and lucidly described in the literature.[2] They can be most simply understood in terms of the minimum momentum transfer to the nucleus. The minimum momentum transfer occurs when the outgoing electron and photon (Fig. 1) are both collinear with the incident electron:

$$q_{min} = q_L \equiv \delta = \frac{m^2}{2E} \frac{x}{1-x}$$

where m is the electron mass.

Thus the minimum momentum transfer is longitudinal, or parallel to the direction of the incident electron. If either of the outgoing particles has transverse momentum, the momentum transfer to the nucleus is increased and in general also has a transverse component. Coherent Bremsstrahlung in a crystal occurs when the total momentum transfer vector $\vec{q}$ equals a characteristic momentum of the reciprocal lattice,[3]

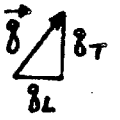

Fig. 2a

$\vec{q} = 2\pi/a\ (H\hat{i} + K\hat{j} + L\hat{k})$, where H, K, L are integers.

We plot a few reciprocal lattice points in momentum space, and consider an electron incident in the 100 direction ($\hat{i}$ axis):

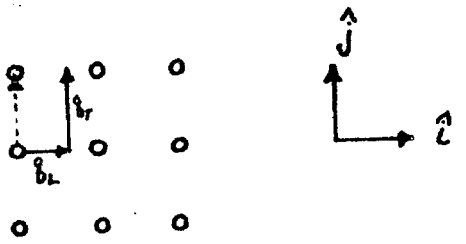

Fig. 2b

For a q_T corresponding to the 010 reciprocal lattice point, coherence can occur at $q_L = 0$ (dashed arrow). This will cause the beam to blow up into an infinity of zero energy photons. Thus the crystal must be tilted so that q can equal a lattice momentum for $q_L \neq 0$.

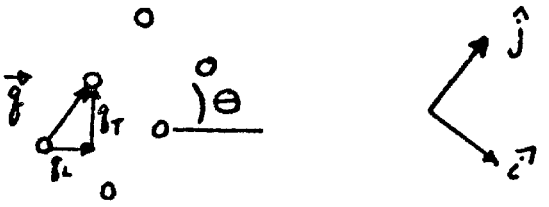

Fig. 3

Obviously, the crystal must be tilted in two directions to avoid the same effect in the other plane (i,k). In terms of the polar and azimuthal angles (θ,ψ) of the rotated crystal i axis about its original direction:

$$q_L = \sin\theta\ (K\cos\psi + L\sin\psi).$$

Typically, the rotation of the crystal is obtained by first aligning the crystal axis with respect to the beam and then tilting the crystal about the horizontal axis by a small angle θ_H and turning it about the vertical axis by a small angle θ_V. In order to prevent ψ from swinging wildly due to small changes in these angles, one of these small angles must be made much larger than the other one.

TYPICAL BEAMS POSSIBLE AT FERMILAB

The equivalent photon spectra from electrons of 150 GeV or 450 GeV incident on a diamond or silicon crystal radiator are shown in Figures 4, 5 & 6. The beam is incident along the 100 axis of the crystals, with the 010 axis at an azimuthal angle of 44.75°. The crystal mount is turned by 200 mrad about the vertical axis and tilted 1.25 mrad about the horizontal axis. For 150 GeV incident a huge coherent peak at x = 0.80 is observed which is about 3.5 times better for diamond than for silicon.

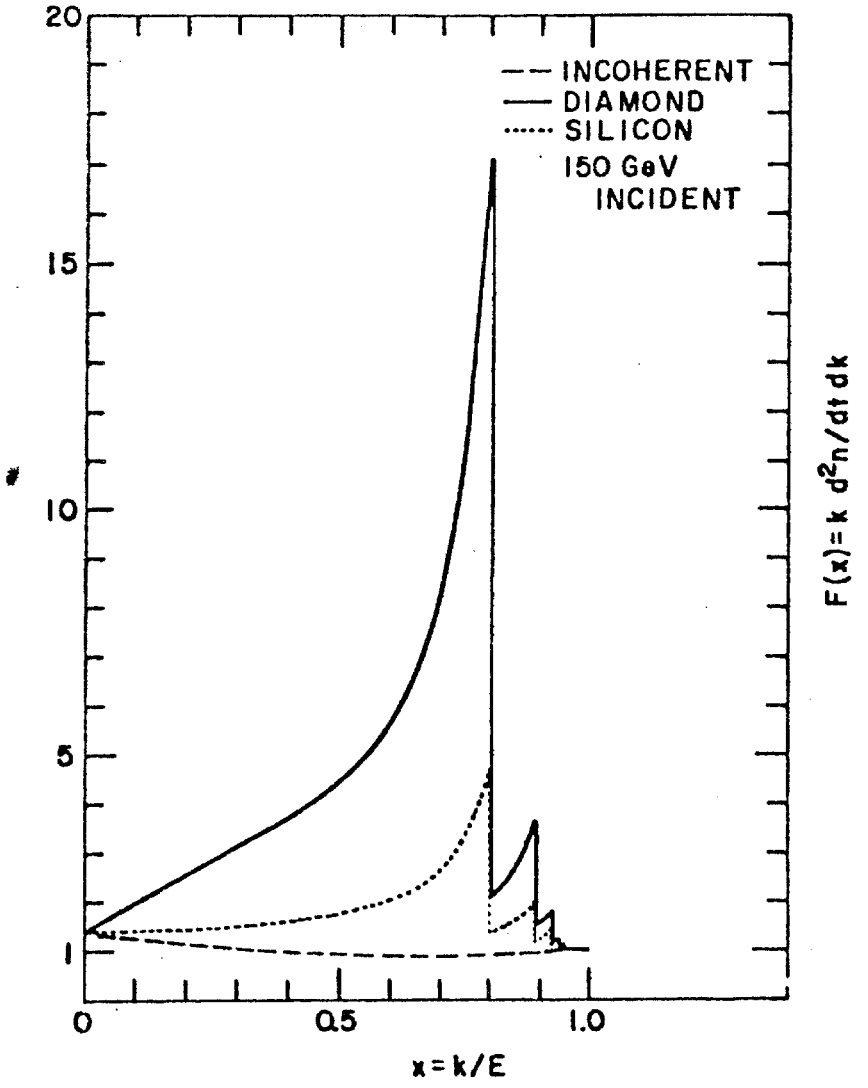

Fig. 4

For 450 GeV electrons the coherent peak remains the same height and moves out to x = 0.92. Neither the angular divergence of the beam nor the mosacity of the crystals has been included in these figures. However, Figure 6 shows the effect of variations of θ_V and θ_H typical of the Fermilab beam divergence.[4] (Table I). The polarization of the beam is given on this figure.

The following conclusions can be drawn:

i) The effect is not sensitive to incident energy and has the nice feature that the x of the coherent peak increases with increasing electron energy so that you win twice. The energy of the coherent photons increases faster than the incident energy.

ii) The effect is very sensitive to the beam angular divergence but is ok at Fermilab if the beam has no tails. Only one angular divergence of the beam is required to be small.

iii) Diamond is 3 times better than silicon. However, the use if a diamond implies that the beam spot size at the radiator must be very small.

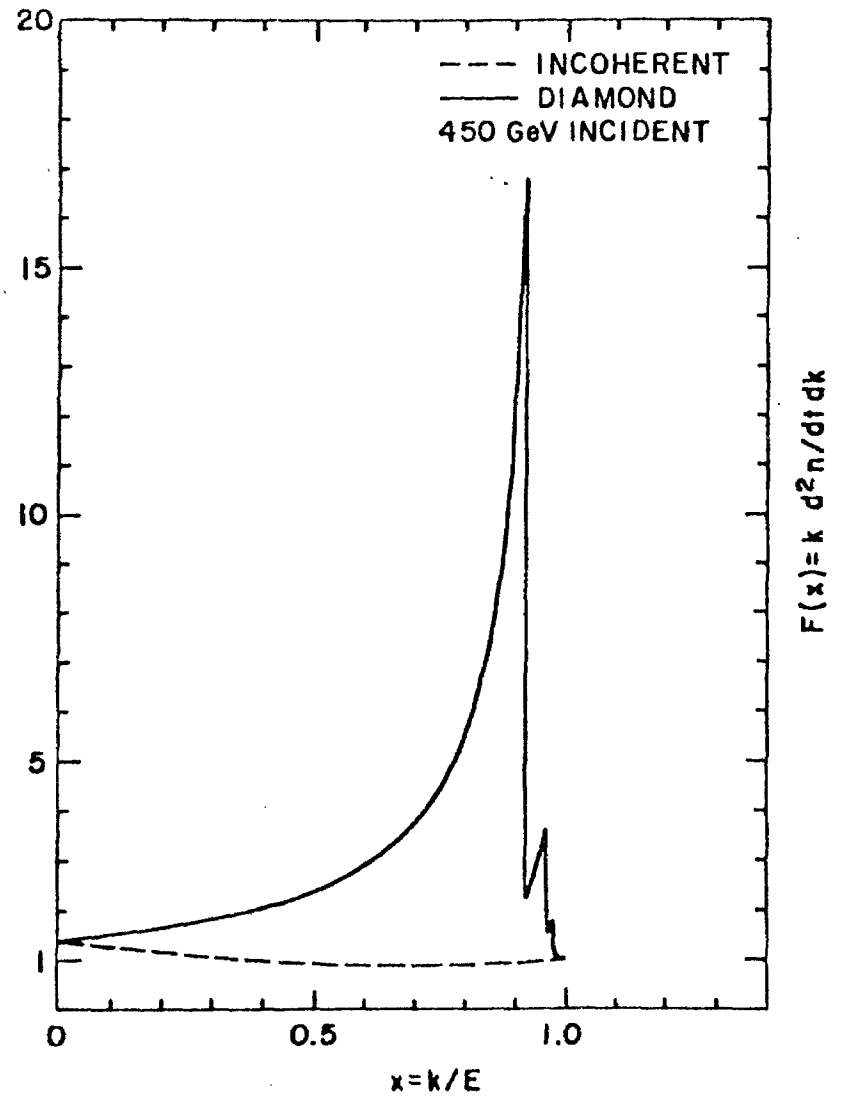

Fig. 5

Table I
Size of Fermilab Electron Beam

	$\Delta\theta$ mrad	Full Size Dimension At Target mm	90' Downstream Equivalent to Full Size At Radiator 90' Upstream mm
DOUBLET			
HORIZ	$\pm$0.44	4.6	25.4
VERT	$\pm$0.14	6.9	6.1
TRIPLET			
HORIZ	$\pm$0.61	8.4	33.9
VERT	$\pm$0.17	8.3	9.0

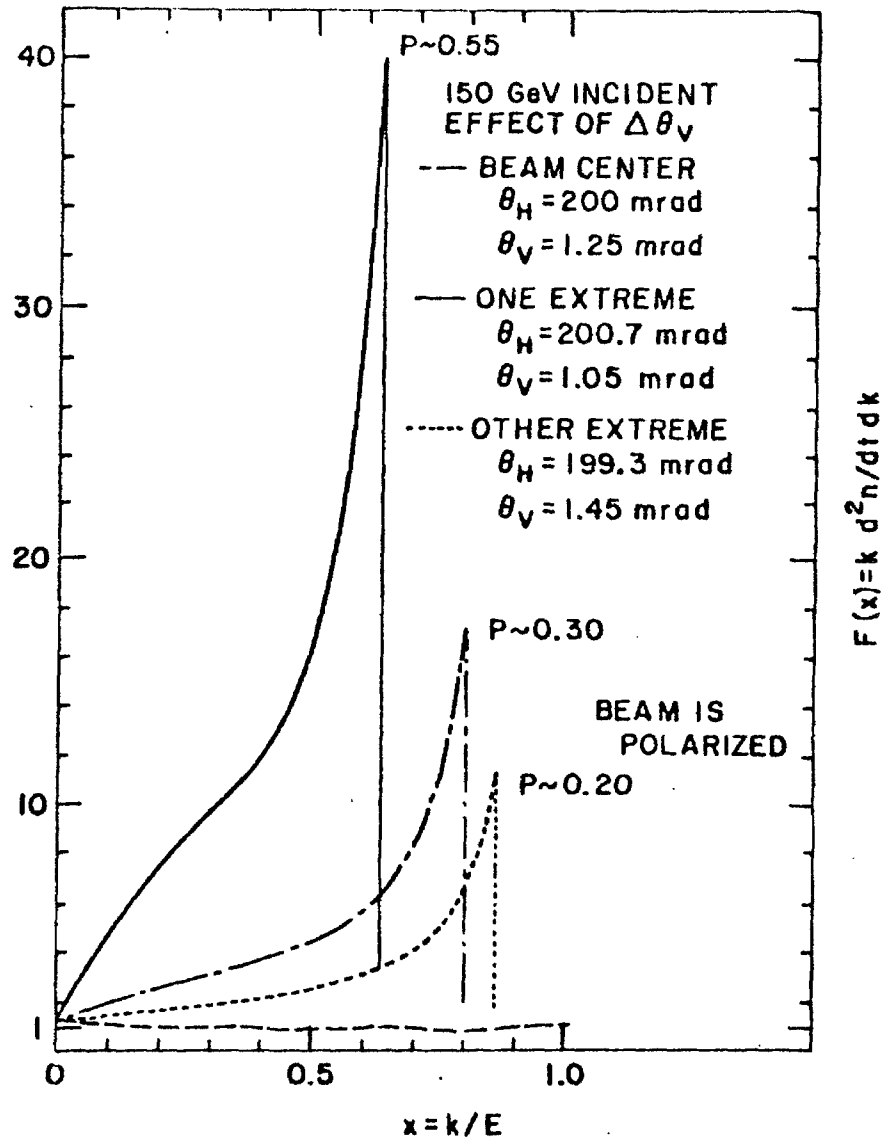

Fig. 6

PRACTICAL CONSIDERATIONS

In order to see what this means in practical terms, an exploded view of a diamond octohedron showing the crystal axes is given in Figure 7. (This fixture comes from Roy Schwitters' thesis.) The sizes of the diamond octahedra as a function of the dimension of an edge are given below.

TABLE II

Sizes of Diamond Octahedra $\rho = 3.53$ 1gm ≈ 5 carats

Edge Dimension mm	Point-to-Point Distance mm	Weight Carats
7.0	9.9	2.85
8.0	11.3	4.26
8.5	12.0	5.11
10.0	14.4	8.32

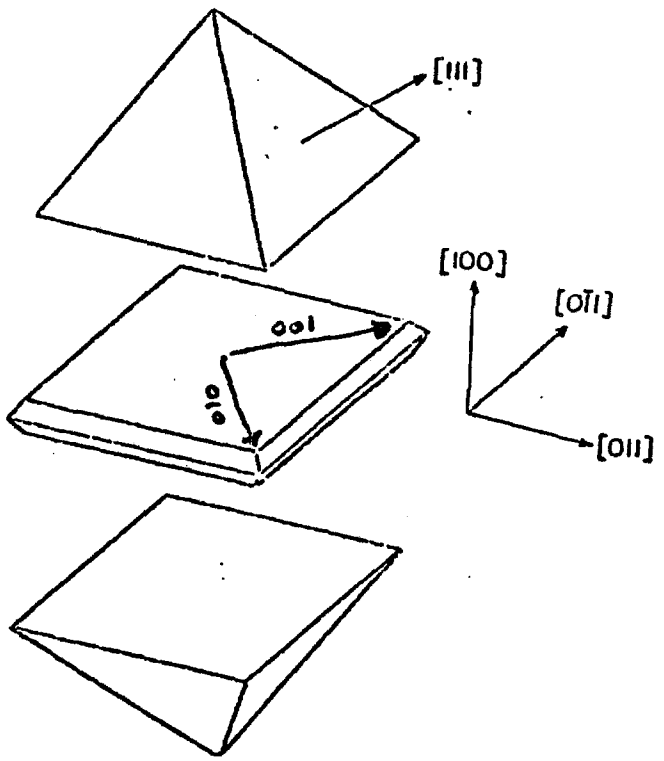

Fig. 7

The most reasonable size is 8.5 mm on an edge or 5.1 carats. Miraculously with the orientation specifed above for Figs. 4, 5, & 6, two such diamonds would be decently matched to the Fermilab beam spot size. A beam eye view of the radiator is:

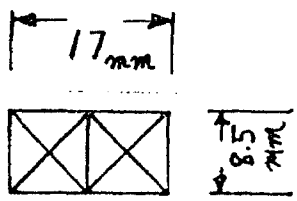

Fig. 8

Note that if the beam could be focused on the radiator instead of on the target (90' further down stream) then only one diamond would be required.

ADVANTAGES OF A COHERENT BEAM

Depending on the exact details of the mosaicity and dimensions of available diamonds, and the spot size of the beam at the radiator, the coherent Bremsstrahlung beam using a diamond radiator might actually produce more high energy photons than obtainable with a conventional thick radiator. For instance the beam shown in Figure 4, with a diamond radiator 6 mm thick, will produce the number of equivalent photons corresponding to an amorphous radiator 0.22 radiation lengths thick, averaged over the whole spectrum. However, the number of high energy equivalent photons, $x > 0.5$, produced corresponds to a 0.30 thick radiator, while the low energy photons $x < 0.5$, corresponds to a 0.12 thick radiator. Note that these values are averaged over the respective x intervals. At the discontinuity point, $x=0$, there is no coherent enhancement so the radiator appears to have its incoherent thickness of 0.05 radiation lengths. If the degrading[1] of the beam is governed only by the apparent radiation length at $x = 0$, then the thick target Bremsstrahlung corrections for the coherent beam will be much less than the thick target corrections for amorphous radiators. This point remains to be checked quantitatively.

In summary, the coherent photon beam at Fermilab energies has three nice features when compared to conventional beams:

i) The photon spectrum is strongly peaked at high energy.
ii) There are fewer low energy photons per high energy photon by a large factor.
iii) The photons in the coherent peak are linearly polarized.

PHYSICS PROGRAMME

My original motivation for trying to obtain increased yields of high energy photons, was to study "hard" or large transverse momentum processes induced by photons. In proton-proton collisions, particle production at large transverse momentum (P_T) has a very strong center-of- mass energy ($\sqrt{s}$) dependence.[5] The invariant cross section for inclusive π° production near 90° in the c-m system follows the form

$$E\frac{d^3\sigma}{dP^3} \sim P_T^{-8.6}\,(1-x_T)^{10.6} \quad \text{For} \quad 3 \le P_T \le 7 \text{ GeV/c}$$

and

$$\sim P_T^{-5.1}\,(1-x_T)^{12.1} \quad \text{For } 7.5 \le P_T \le 14 \text{ GeV/c}$$

where $x_T = 2P_T/\sqrt{s}$. The x_T dependence is characteristic of the structure functions of the constituents in both protons while the P_T dependence is characteristic of the force law governing the constituent scattering.

A very important issue in hadron initiated large P_T reactions is whether and how often direct single γ rays are produced. The experiments[5] are very difficult because of the fierce background of photons from the decays of the more dominantly produced hadrons. The theoretical interest arises from the prediction[6] of the constituent reaction:

Quark + Gluon -------→ Quark + Photon
Also known as the "QCD Compton Effect"

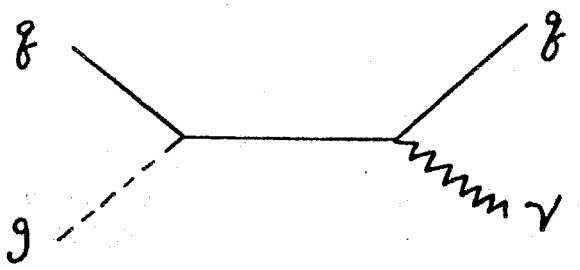

Fig. 9

The exact same reaction can be studied using incident photons. The principal advantage is that you are certain of the identity of the incident photon. Parenthetically, the field of large P_T reactions initiated by photons has hardly, if at all, been studied.

In the jargon of the field[7], there are two classes of photon initiated large P_T events: three jet events and four jet events. The three jet events represent the QCD Compton effect:

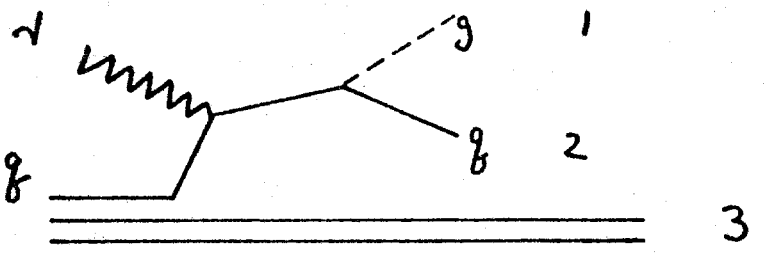

Fig. 10

The four jet events come from the "photon structure function", i.e., the photon acts like a source of q $\bar{q}$ pairs:

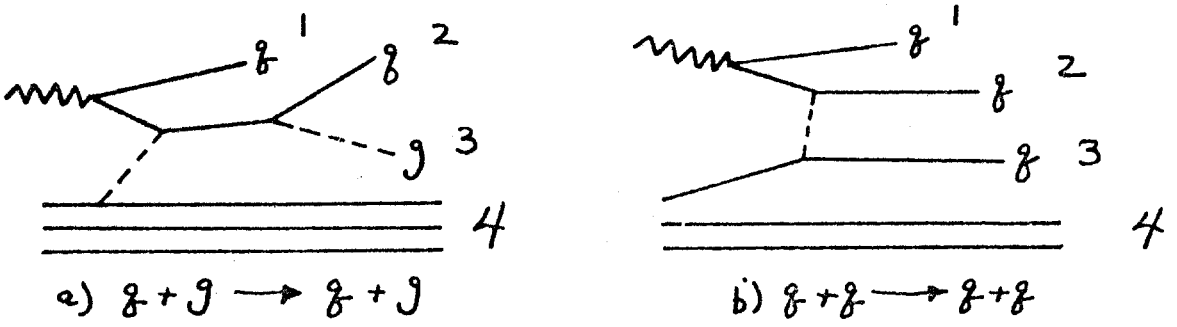

Fig. 11

In Fig. 11a) a quark from the photon structure function scatters from a gluon inside the nucleon; in Fig. 11b a quark from the photon scatters from a quark in the nucleon. Obviously there are even more complicated topologies to consider. Note that in Figures 11a and b the lines labelled 2 and 3 represent high P_T jets while lines 1 and 4 represent low P_T beam and target jets. In the three jet events of Figure 10, the beam jet is absent.

Owens[7] has calculated the cross sections for these reactions in great detail. I have taken the liberty of parameterizing his calculations for jet production by photons near 90° c-m by the simple form:

$$E\frac{d^3\sigma}{dp_3} \cong 1.8 \times 10^{-29} \text{ cm}^2/\text{GeV}^2 \; P_T^{-5.1} \; (1-x_T)^{2.5}$$

The predicted $\sqrt{s}$ dependence is much less than that observed in proton-proton collisions and is a consequence of the pointlike nature of the photon. If this slow $\sqrt{s}$ dependence were indeed observed, it would be a marvelous confirmation of the theory but would also have the practical consequence of lessening the need for the highest energy photons and thus allowing higher rates and higher polarizations to be achieved.

The three-jet events test QCD in a very fundamental way and have several very important properties. If the incident photon energy is known, then the kinematics of the two high P_T jets is constrained so that the 3-jet events can be uniquely separated from the 4-jet events. If the QCD constituent Compton cross section is considered as "known", then the proton structure function can be determined from the observed rate of 3-jet events. (Or vice versa.) Finally, and most relevant to this conference, there are polarization effects which are said to provide "A rigorous test of perturbative QCD as well as an important check on the color hypotheses".[8]

In QED, the well known effect in pair production by polarized photons is that the plane of the produced e^+e^- pair tends to lie parallel to the plane of the incident photon polarization. In QCD, all the polarization effects are said[8] to vanish in lowest order to the extent that the quark mass is zero. Thus, QCD polarization effects are sensitive to higher order processes, in particular the three-gluon coupling, and are predicted[8] to be opposite in sign to the QED correlation.

For reactions like charmed particle pair photoproduction which involve heavy quarks[9], lowest order polarization effects are large and provide different QCD tests. For vector gluons, the asymmetry correlation is like QED, for scalar gluons it has the opposite sign, and for pseudoscalar gluons it is zero.[9] Regardless of the theoretical details[10] the observation of a correlation between the electric field direction of an incident photon and the plane of outgoing hadron states from a "hard" collision would be striking confirmation of the constituent composition of protons and the intimate connection between electromagnetism and strong interactions.

ACKNOWLEDGMENTS

I would like to thank Greg Snow for help in the early stages of this work. The equivalent photon spectra were calculated with the help of a computer program originally written by Roy Schwitters. I would also like to acknowledge enlightening conversations with Roy Schwitters, Peter Bussey, Charlie Sinclair, Lou Osborne, Dieter Walz, and Leon Madansky.

REFERENCES

1. Y.S. Tsai and V. Whitis, Phys. Rev. 149, 1248 (1966).
2. G. Diambrini-Palazzi, Rev. Mod. Phys. 40, 611 (1968) and references quoted therein; U. Timm, Fortschritte der Physik 17, 765 (1969); D. Luckey and R.F. Schwitters, NIM 81, 164 (1970); R. Schwitters, SLAC-TN-70-32 (1970); G. Diambrini-Palazzi and A. Santroni, 300 Gev Working Group, CERN/ECFA/72/4, Vol. I, p. 231; C.A. Heusch, U.C.S.C. 76-056 (1976); BCGLMRS Proposal CERN/SPSC/78-42, SPSC/P 102 (1978); CERN Bulletin No. 21/78, 22 May 1978.
3. G. Diambrini-Palazzi, Nuovo Cimento Suppl. 25X, 88 (1962); G. Barbiellini, G. Bologna, G. Diambrini and G.P. Murtas, Phys. Rev. Letters 8, 112 and 454 (1962); see also, H. Uberall, Phys. Rev. 103, 1055 (1956) and references quoted herein.
4. P.H. Garbincius, Report in preparation; C. Haliwell, et. al., FN-241 (1972).
5. For a review of Hardon Physics at high P_T see M.J. Tannenbaum in Particles and Fields-1979, Proceedings of the APS Division of Particles and Fields meeting, Montreal, P.Q., Canada, October 1979.
6. H. Fritzsch and P. Minkowski, Phys. Lett. 69B, 316 (1977).
7. J.F. Owens, Phys. Rev. D21, 54 (1980); C.H. Llewellyn Smith, Phys. Lett. 79B, 83 (1978).
8. A. DeVoto, J. Pumplin, W. Repko and G.L Kane, Phys. Rev. Letters 43, 1062 (1979).
9. D.W. Duke and J.F. Owens, Phys. Rev. Letters 44, 1173 (1980).
10. Note that Stan Brodsky at this conference disagreed with some of the conclusions of reference 8.

FERMILAB-Proposal-0670

ADDENDUM TO PROPOSAL P-670

T.J. Chapin, R.L. Cool, K. Goulianos*, K. Jenkins,
G.R. Snow, H. Sticker and S.N. White

The Rockefeller University
New York, NY 10021

SUMMARY

We propose to extend the study of inclusive pion and photon diffraction dissociation to 300 GeV, and study small t pion elastic scattering from 50 to 300 GeV, using our E-612 apparatus in its present set-up in the Tagged Photon Laboratory during the second part of the 1983-1984 running period.

*Spokesman (Telephone: 212/570-8827)

Proposal P-670 discusses the continuation of experiment E-612 at the Tevatron. At the time P-670 was submitted, we only indicated the general direction in which we would continue the experiment and stated that we would be more specific when results from E-612 became available. About one-half of our E-612 data have now been analyzed and our results are presented in a paper[1] entitled "Diffraction Dissociation and the Direct Hadronic Interaction of the Photon". In view of these results, we propose to study pion and photon dissociation at energies up to 300 GeV. The TPL beam line is equipped to deliver electrons of this energy. The electrons are produced by intercepting a secondary neutral beam with a thin radiator. In E-612, the pion beam was formed by replacing the radiator with four inches of lead. This beam was accompanied with an electro-magnetic halo, which limited the flux of pions that could be accepted by the apparatus to $\sim 5 \times 10^4$ per pulse. In order to decrease the background accompanying the pions, we propose to run with a pion beam which is produced directly from the primary protons. We understand that this can be done at little expense. An added advantage of this method is that the required primary beam intensity will be small.

The main purpose of the proposed study is to understand better our E-612 results on the finite mass sum rule (FMSR) and factorization. At twice the energy, the M_X^2 extent of the diffractive region doubles. Hence, the high mass $1/M_X^2$ behavior will be checked better and a more reliable extrapolation into the low mass region will be made. It will be interesting to test the FMSR at various values of t. The importance of this test in

relation to "the shape of the ρ" has been emphasized in our paper[1]. The test of factorization in our E-612 experiment does not give an accurate value of the "effective photon mass", M_0. We would like to perform this test well and compare the value of M_0 with that obtained from the FMSR.

The charged multiplicity distributions of pion and photon diffractive masses will be measured up to $M_X^2 = 0.1s = 56\ GeV^2$. Direct comparison of the charged multiplicities provides a test of the universality hypothesis[2].

In the course of the above study, small t pion elastic scattering will also be measured. The world data on the slope parameter of π^-p elastic scattering at $|t| \sim 0.05\ (GeV/c)^2$, shown[3] in Figure 1, are not good enough to allow a definite conclusion to be drawn about the equality of the increase of the slope parameter with energy for π^-p and pp elastic scattering. We propose to measure b for $\pi^-p \to \pi^-p$ at energies from 50 to 300 GeV. Even in the presence of possible small systematic errors, such a measurement will give the correct energy dependence of the slope.

In determining the desired length of the proposed run, the quality of the beam is a key factor. We feel that, with a good pion beam and a photon beam similar to the one we had in E-612, an amount of time comparable to that spent in E-612 would be required; i.e., about two to three months. Thus, the second half of the 1983-1984 running period indicated "OPEN" for TPL in the 11/13/82 tentative schedule, should be sufficient. If the high energy tagged photon beam intensity is not high enough during this period. we intend to ask for more time in the second half of the 1984-1985 running period to complete the photon part of the experiment.

REFERENCES

1. T. Chapin et al., "Diffraction Dissociation and The Direct Hadronic Interaction of the Photon".
2. K. Goulianos, "Diffractive Interactions of Hadrons at High Energies." (Contributed paper at The International Conference on High Energy Physics, Paris, France, July 26-31, 1982 - Rockefeller University Report No. RU 81/A-23.
3. K. Goulianos et al., "Universality of Charged Multiplicity Distributions," Phys. Rev. Letters 48, 1454 (1982).

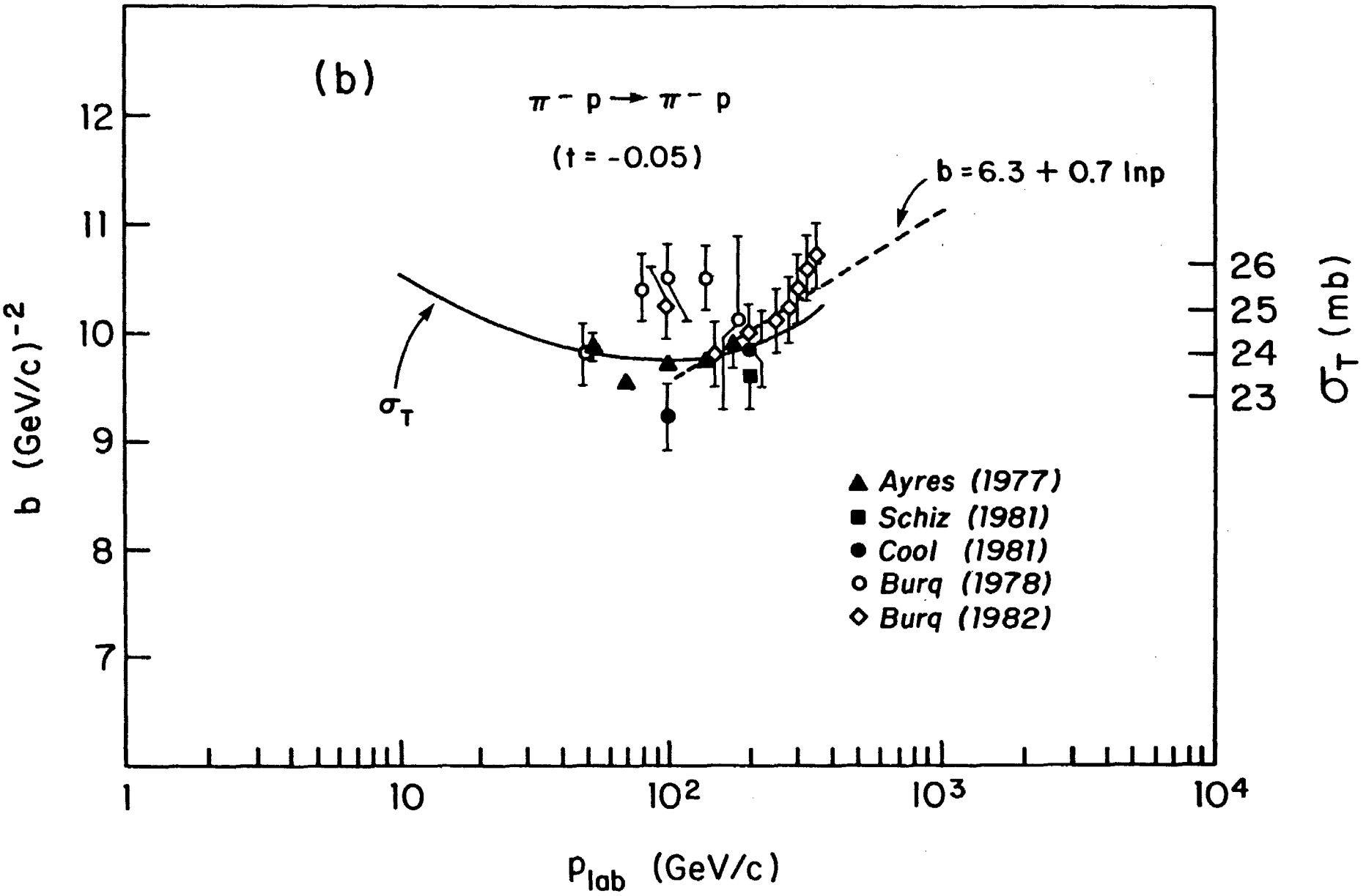

FIG. 1 - Slope parameter of $\pi^- p \rightarrow \pi^- p$ at $|t| \sim 0.05$ (GeV/c)^2 as a function of laboratory momentum (from Reference 2).

DIFFRACTION DISSOCIATION and THE DIRECT HADRONIC INTERACTION OF THE PHOTON

K. Goulianos*

The Rockefeller University
New York, N.Y. 10021, U.S.A.

Invited paper presented at
The XVIIIth Rencontre de Moriond on Gluons and Hadron Physics
Session 1, January 23-29, 1983
La Plagne, Savoie, France

ABSTRACT

We report a measurement of the inclusive diffraction dissociation cross section of $\sim$ 100 GeV photons on hydrogen; we test the finite mass sum rule and, comparing with pion dissociation data, we test factorization. Our results are interpreted as providing a measurement of the direct, non "vector-meson dominance" hadronic interaction of the photon.

*Report on Fermilab Experiment E-612:

T. Chapin, R. Cool, K. Goulianos, K. Jenkins,
J. Silverman, G. Snow, H. Sticker and S. White

The Rockefeller University
New York, N.Y. 10021, U.S.A.

and

Yue Hua Chou
Institute of High Energy Physics, Beijing
The People's Republic of China

In an experiment performed at Fermilab, E-612, we measured the inclusive diffraction dissociation cross section $d^2\sigma/dtdM_X^2$ of $\sim$100 GeV photons incident on protons,

$$\gamma + p \rightarrow X + p \tag{1}$$

in the kinematic range $0.02 < |t| < 0.1$ $(GeV/c)^2$ and $M_X^2/s \lesssim 0.1$. As a control experiment, we also measured, in the same apparatus, the pion diffraction dissociation cross section,

$$\pi^- + p \rightarrow X + p \tag{2}$$

at 100 GeV/c. Pion dissociation has been measured previously[1]; this experiment represents the first measurement of inclusive photon dissociation at high energies.

We find that, for $M_X^2 > 4$ GeV^2, the differential cross sections for both reactions vary as $1/M_X^2$ and are exponential in t, a behavior consistent with that predicted by a simple triple-Pomeron Regge type amplitude. By applying the finite mass sum rule to the photon data, and by comparing the photon with the pion data to test factorization, we conclude that the photon has a direct hadronic interaction in addition to that described by the well known[2] vector-meson dominance model (VDM).

The experiment was performed in the tagged photon beam of Fermilab. The photons were obtained from an 148 GeV/c electron beam incident on a 20% tungsten radiator. The energy of the photons was determined to $\pm 2\%$ by bending the radiating electrons out of the beam and measuring their energy with lead glass counters. Typically, the photon beam contained

$\sim 1 \times 10^6$ tagged photons per pulse in the energy range $75 < E_\gamma < 148$ GeV. With the Bremsstrahlung energy spectrum varying as 1/E, the mean energy of the photons was ~ 100 GeV. The photon flux was limited by the rate capability of our detector. Double photon production in the radiator was monitored by a total absorption counter which, placed in the photon beam downstream of our apparatus, measured the total energy of the non-interacting photons. The pion beam was formed by intercepting the secondary neutral beam, which created the electrons, with a 5 cm lead brick. An electromagnetic halo accompanying the beam limited the acceptable flux of pions to $\sim 5 \times 10^4$ per pulse. The pulse repetition period of the machine was ~ 10 sec and the beam spill time ~ 1 sec. Data were collected in two runs of approximately equal duration, one during the month of January and the other during March of 1982.

The experimental technique consisted in measuring the kinetic energy and polar angle of recoil protons in the region $10 < T < 50$ MeV and $45^0 < \theta < 90^0$. The variables t and M_x^2 were then determined from T, θ and p_o, the momentum of the beam particle, using the equations

$$t = -2M_p T \tag{3}$$

$$M_x^2 = M_o^2 + 2p_o \sqrt{|t|} \ (\cos\theta - \sqrt{|t|}/2M_p) \tag{4}$$

where M_p is the mass of the recoil proton and M_o the mass of the incident particle.

The apparatus, TREAD (The Recoil Energy and Angle Detector), shown in Figure 1, was described in detail in a previous publication[3]. It is a hydrogen filled, high pressure time projection chamber (TPC) that served

both as target and as detector of the recoil protons. It consists of two cylindrical drift regions in tandem, each 45 cm in diameter and 75 cm long. The beam entered the TPC alaong the axis of the cylinder through a 0.75 mm thick, 5 cm dia. beryllium window and exited through a 2 mm thick, 20 cm dia. aluminum window. The dissociation products also exited through the aluminum window, whereupon their charged multiplicity was determined by measuring the pulse height in two scintillation counters. This technique was used previously[4] by some members of this group in a hadron experiment, E-396, performed at Fermilab's meson laboratory. The energy of the recoil protons was determined by stopping them in 2.5 cm thick plastic scintillation counters located inside the pressure vessel. The energy loss in the hydrogen gas, dE/dx, was obtained from the pulse height of the sense wires. Recoiling protons were identified by comparing T with dE/dx.

In this report we present the result of the analysis of the data collected during March 1982. The data obtained in January of 1982 are currently being analyzed. Details of the analysis will be given elsewhere[5]. Basically, after track selection and appropriate cuts in dE/dx versus E and in recoil time of flight, the background was negligible.

Figure 2 is a scatter plot of the recoil kinetic energy against dE/dx for the photon data. The prominent band represents the recoil protons for which the energy loss varies as 1/T. Multiplying dE/dx by T yields a constant which is proportional to the mass of the recoil particle. Figure 3 is a histogram of (dE/dx) · T. The peak consists of recoil protons. Its width is mainly due to the dE/dx measurement resolution.

The M_X^2 distributions of the pion and photon data, normalized respectively to the $\pi^- p$ and γp total cross sections, are shown in Figure 4. The data, representing about 7,500 pion and 8,500 photon events, are plotted against the cross-symmetric variable ν ,

$$\nu = M_X^2 - M_o^2 - t \tag{5}$$

where M_o is the mass of the incident particle. The width of the pion elastic peak at $\nu \cong 0$ and of the ρ-meson peak at $\nu \cong 0.6$ GeV^2 are mostly due to the measurement resolution. The resolution is poorer in the photon data, which were collected over a period of one month, than in the pion data, collected during one day. In the Regge model, under the assumption of factorization, the high mass diffraction dissociation cross-section arising from a triple-Pomeron term can be written as

$$\frac{d^2\sigma^{hp}}{dtd\nu} = \frac{\beta_{hP}(o) \quad \beta^2{}_{pP}(t) \quad G_{PPP}(t)}{16\pi\nu} \tag{6}$$

where h represents the hadron dissociating on the proton and P represents the Pomeron. In the same model, the total cross section at high energies is given by

$$\sigma_T^{hp} = \beta_{hP}\,(o) \quad \beta_{pP}\,(o) \tag{7}$$

In writing (6) and (7), we have taken, for simplicity, the Pomeron trajectory to be $\alpha(o) = 1$ and, because of our small t values, the slope of the trajectory to be $\alpha'(t) = 0$. The ratio of the diffractive to the total cross section,

$$\frac{d^2\sigma^{hp}/dt\ d\nu}{\sigma_T^{hp}} = \frac{\beta_{pP}^2(t)}{\beta_{pP}(o)} \quad \frac{G_{PPP}(t)}{16\pi\nu} \tag{8}$$

is independent of the incident particle type. The $1/\nu$ behavior predicted by Eq. (6) and the scaling of the diffractive to the total cross section given by Eq. (8) have been found to hold for $\pi^{\pm}$, $K^{\pm}$, and $p^{\pm}$ hadrons dissociating on protons[1]. Figure 4 shows that the high mass diffractive photon cross section is $\sim$15% higher than the pion cross section (scaled by the corresponding σ_T). This could, of course, be considered as a positive test of factorization in view of the fact that the photon total cross section is $\sim$200 times smaller than the pion cross section. However, this discrepancy finds a logical explanation in the framework of the vector-meson dominance model.

In its original version, the VDM states that the hadronic interaction of the photon is transmitted through the coupling of the photon to the vector mesons ρ, ω and ϕ. For simplicity, we will consider only the ρ-meson in this discussion. A photon cannot transform into a ρ in free space. Conversion to ρ requires an energy change $\Delta E = M_\rho^2/2E_\gamma$. For 100 GeV photons, ΔE = 3 MeV. Through the uncertainty principle, $\Delta E \cdot \Delta t \sim 1$, this energy shift corresponds to a time interval which is large compared to the characteristic time of strong interactions set by the mass of the pion (140 MeV). Thus, high energy photons can live in and interact with nuclear matter as "free" ρ-mesons. Of course, photons can also interact directly. Therefore, the effective "incident photon" mass, M_0^2, lies somewhere between zero and M_ρ^2. Assuming that there is no interference between the γ and ρ amplitudes, the value of M_0^2 is given by

$$M_o^2 = \frac{P_\gamma \sigma_\gamma^D M_\gamma^2 + P_\rho \sigma_\rho M_\rho^2}{P_\gamma \sigma_\gamma^D + P_\rho \sigma_\rho} = \frac{P_\rho \sigma_\rho M_\rho^2}{\sigma_\gamma^T} \qquad (9)$$

where $P_{\gamma,\rho}$ are the probabilities of finding the photon in the $\gamma(M_\gamma^2 = 0)$ or $\rho(M_\rho^2 = 0.59\ \text{GeV}^2)$ states and σ_γ^D is the "direct" γ total cross section. The VDM assumes that $P_\rho \sigma_\rho >> P_\gamma \sigma_\gamma$ and hence $M_o^2 \cong M_\rho^2$. Had we used M_ρ^2 instead of M_γ^2 in Figure 4, the photon data would be in agreement with the pion data. Thus, assuming the validity of factorization and of the Regge model, this result supports the VDM. However, it is not sensitive enough to rule out a direct photon interaction of $\sim 20\%$ which is required to explain the shadowing of photons in nuclei[2]. Such an interaction is also desirable in the simple VDM which can account for only $\sim 80\%$ of the photon total cross section, although this inadequacy can be corrected by introducing the generalized VDM[2]. A more sensitive measurement of M_o^2, and hence of the direct photon interaction, is provided by our data through the application of the finite mass sum rule (FMSR).

The FMSR[6] relates the high mass diffractive cross section to the low mass "resonance region." It states that the fit to the large ν differential cross section, $d^2\sigma/dtd\nu$, multiplied by ν represents the average behavior of $\nu(d^2\sigma/dtd\nu)$ in the low mass region, including elastic scattering for which $\nu = |t|$:

$$|t| \frac{d\sigma_{e\ell}}{dt} + \int_0^{\nu'} \nu \frac{d^2\sigma}{dtd\nu} d\nu = \int_0^{\nu'} \nu \left(\frac{d^2\sigma}{dtd\nu}\right)_{\text{fit at large } \nu} d\nu \qquad (10)$$

The value of ν' must lie beyond the "resonance region" but is otherwise arbitrary. However, the lower the value of ν' the more sensitive the test of the FMSR. The elastic contribution appears explicitly in Eq. (10). Experimentally, due to resolution in the measurement of M_X^2, elastic scattering appear as a peak of finite width in ν centered around $\nu = |t|$. In applying the FMSR, the elastic events can be treated just as the inelastic ones; namely, by multiplying the apparent cross section $d^2\sigma/dtd\nu$ by $\nu = M_X^2 - M_O^2 + |t|$ and integrating over ν down to values which are low enough to include all events. For a resolution broadened peak which is symmetric around $M_X = M_O$, the elastic events in this procedure are, in effect, multiplied by $|t|$, as required by the FMSR. Thus, in applying the FMSR to experimental data, Eq. (10) can be written as

$$R \equiv \frac{\int_{\text{fit at large } \nu}^{\nu'} \nu \frac{d^2\sigma}{dtd\nu} \, d\nu}{\int_{O}^{\nu'} \nu \left(\frac{d^2\sigma}{dtd\nu}\right) \, d\nu} = 1 \qquad (11)$$

where the lower limit of integration in the numerator has been omitted but it is understood that one must sum over all events below ν', including the elastic events that are forced by the resolution to appear at negative values of ν.

Figures 5a and 5b show $\nu(d^2\sigma/dtd\nu)$ for our pion and photon data plotted against $\nu = M_X^2 - M_{\pi,\gamma}^2 + |t|$. For $\nu \gtrsim 4$ GeV, our data for both reactions are flat, implying an $1/\nu$ behavior of $d^2\sigma/dtd\nu$ and hence

triple-Pomeron dominance in the diffractive cross sections. The $A_1(M^2=1.63)$ and ρ' $(M^2=2.56)$ peaks are clearly visible in the pion and photon data, respectively. Applying the FMSR with $\nu' = 4$ GeV^2, we find $R_\pi = 1.10 \pm 0.05$ and $R_\gamma = 1.43 \pm 0.04$. Clearly, in this straightforward application, the FMSR fails for the photon data. We attribute this failure to the fact that, as discussed previously, the photon interacts partly as a ρ-meson and therefore $\nu = M_X^2 - M_0^2 - t$, where M_0^2 is given by Eq. (9). Treating M_0^2 as a free parameter and demanding the validity of the FMSR, i.e., $R = 1$ in Eq. (10), we find $M_0^2 = 0.46 \pm 0.02$ GeV^2. From Eq. (9), we then find $P_\rho \sigma_\rho / \sigma_\gamma^T = M_0^2/M_\rho^2 = (0.46 \pm 0.02)/0.59 = 0.78 \pm 0.035$ and consequently

$$\sigma_\gamma^D = (0.22 \pm 0.035)\, \sigma_\gamma^T \qquad (12)$$

i.e., the direct hadronic photon cross section is 22 ± 3.5% of the total. As mentioned earlier, this value is in agreement with results on shadowing of photon total cross sections in nuclei and with the fact that the simple VDM accounts for only $\sim$80% of the total photon cross section.

The t distributions were fitted to the simple exponential form e^{bt}. Figure 6 shows the slope parameter b as a function of M_X^2. The pion elastic scattering and high mass diffraction slopes are in good agreement with the values of 8.92 ± 0.31 and 4.3 ± 0.7 $(\text{GeV}/c)^{-2}$ measured[7] in experiment E-396. The slope at $M_X^2 \cong 0.8$ GeV^2 was obtained from pion data with charged multiplicity ≥ 3 in order to exclude events from the nearby elastic peak. The large value of the slope in this low mass inelastic region is essential in satisfying the FMSR at small values of t. From Eq. (10), it is

seen that as $|t| \to 0$ the elastic contribution vanishes; however, due to the large value of the slope of the low mass inelastic region, the relative contribution of this region increases at small t and the FMSR is satisfied. Our present data are not accurate enough to provide a stringent test of the FMSR as a function of t. Such a test was performed[8] for $pp \to Xp$; it was found that the slope parameter of the low mass region was indeed high and its magnitude was exactly what was required to satisfy the FMSR.

In examining the slope parameters of the photon dissociation data, we observe the following:

(i) The slopes of the high mass photon and pion data are in agreement.

(ii) The slope at the mass of the ρ-meson ($M_X^2=0.59$) is about one unit higher than the pion elastic scattering slope, although the statistical significance of this difference is not very high.

(iii) There is no increase of the slope in the region $M_X^2 > M_\rho^2$.

The M_X^2 dependence of b does not follow exactly the pattern set by the hadron data. The slope is not higher in the region just above the ρ mass and, in this sense, the ρ' does not correspond to the A_1 enhancement.

Following the argument presented previously, it would then appear that the FMSR would be violated at small values of t. However, data from experiments at lower energies (see Fig. 7) indicate that the slope in the mass region $M_X^2 < M_\rho^2$ is higher than the slope of the ρ. Our experimental resolution does not permit us to observe directly this increase of slope at low masses, but indirect evidence is provided by the fact that the measured

slope of the ρ is larger than that of pion elastic scattering. Thus, the low mass "tail" of the ρ in $\gamma p \to Xp$ may indeed play the role of the A_1 and N^* (1400) enhancements observed in $\pi p \to Xp$ and $pp \to Xp$, respectively.

As menionted earlier, we also measured in this experiment the pulse height in two scintillation counters placed downstream of TREAD in order to determine the charged multiplicity of the dissociation products. Figure 8 shows the pulse height spectra for the photon and pion data in the region $3 < M_X^2 < 10$ GeV^2 in units corresponding to minimum ionizing particles. In order to extract the multiplicity distribution, these spectra must be fitted with appropriate Landau functions. However, a direct comparison of the photon and pion data, which in Figure 8 are normalized to the same number of events, already shows that the charged multiplicity distribution has the same mean value and the same width for both reactions. This result is in agreement with the "Universality of Charged Multiplicity Distributions" shown to hold for hadronic masses[9].

In summary, we find that $d^2\sigma/dtd\nu$ for $\gamma(\pi^-) + p \to X + p$ at 100 GeV/c varies as $(1/\nu)\, e^{bt}$, in agreement with a triple-Pomeron amplitude; by testing factorization and the FMSR, we conclude that the effective mass of the incident photon is $M_0^2 = 0.46 \pm 0.02$ GeV^2 and, by comparing with M_ρ^2, we determine the direct, non-VDM hadronic cross section of the photon to be 22 ± 3.5% of the total cross section; from a study of the t-distributions, combined with results from experiments at lower energies, we argue that the low mass "tail" of the ρ-meson is the counterpart of the low mass enhancements A_1 and N^* (1400) observed in $\pi^-(p) + p \to X + p$; finally, from the pulse height spectra in the "multiplicity counters", we verify the universality character of the charged multiplicity distributions for the case of photons.

REFERENCES

1. R.L. Cool, K. Goulianos, S.L. Segler, H. Sticker and S.N. White, Phys. Rev. Letters 47, 701 (1981).
2. T.H. Bauer, D. Spital, D.R. Yennine and F.M. Pipkin, Reviews of Modern Physics 50, 26, (1978).
3. T. Chapin et al., Nuclear Instruments and Methods 197, 305 (1982).
4. R.L. Cool, K. Goulianos, S.L. Segler, H. Sticker and S.N. White, Phys. Rev. Letters 48, 1451 (1982).
5. Gregory Snow, Ph.D. Thesis, Rockefeller University (in preparation).
6. A.I. Sanda, Phys. Rev. D6, 280 (1972); M.B. Einhorn, J. Ellis and J. Finkelstein, ibid. 5, 2063 (1972).
7. R.L. Cool, K. Goulianos, S.L. Segler, G. Snow, H. Sticker and S.N. White Phys. Rev. D24, 2821 (1981).
8. Y. Akinov et al., Phys. Rev. D14, 3148 (1976)
9. K. Goulianos, H. Sticker and S.N. White, Phys. Rev. Letters 48, 1454 (1982).

FIGURE CAPTIONS

FIG. 1 - TREAD (The Recoil Energy and Angle Detector).

FIG. 2 - Recoil particle energy loss, dE/dx, versus kinetic energy. The prominent band represents recoil protons.

FIG. 3 - Recoil particle energy loss times kinetic energy, $(dE/dx)\cdot T$. This product is proportional to the mass of the recoil particle. The position of the peak is normalized to unity so that the abseissa represents M(recoil)/M(proton).

FIG. 4 - M_X^2 distributions for $\gamma(\pi^-) + p \to X + p$ at 100 GeV/c and $0.02 < |t| < 0.1$ $(GeV/c)^2$, normalized to the corresponding total cross sections, $\gamma(\pi^-) + p \to$ anything.

FIG. 5 - Test of the finite mass sum rule: The product $\nu(d^2\sigma/dtd\nu)$, where $\nu = M_X^2 - M_{\pi,\gamma}^2 + |t|$, plotted against ν (a) for $\pi^- p \to Xp$ and (b) for $\gamma p \to Xp$ at 100 GeV/c and $0.02 < |t| < 0.1$ $(GeV/c)^2$.

FIG. 6 - The slope parameter b as a function of M_X^2 for $\gamma(\pi^-) + p \to X + p$ at 100 GeV/c and $0.02 < |t| < 0.1$ $(GeV/c)^2$.

FIG. 7 - The "shape of the ρ" as a function of t (from Reference 2).

FIG. 8 - Pulse height spectra ("charged multiplicities") of the dissociation products for $\gamma(\pi^-) + p \to X + p$ at 100 GeV/c in the region $3 < M_X^2 < 10$ GeV^2.

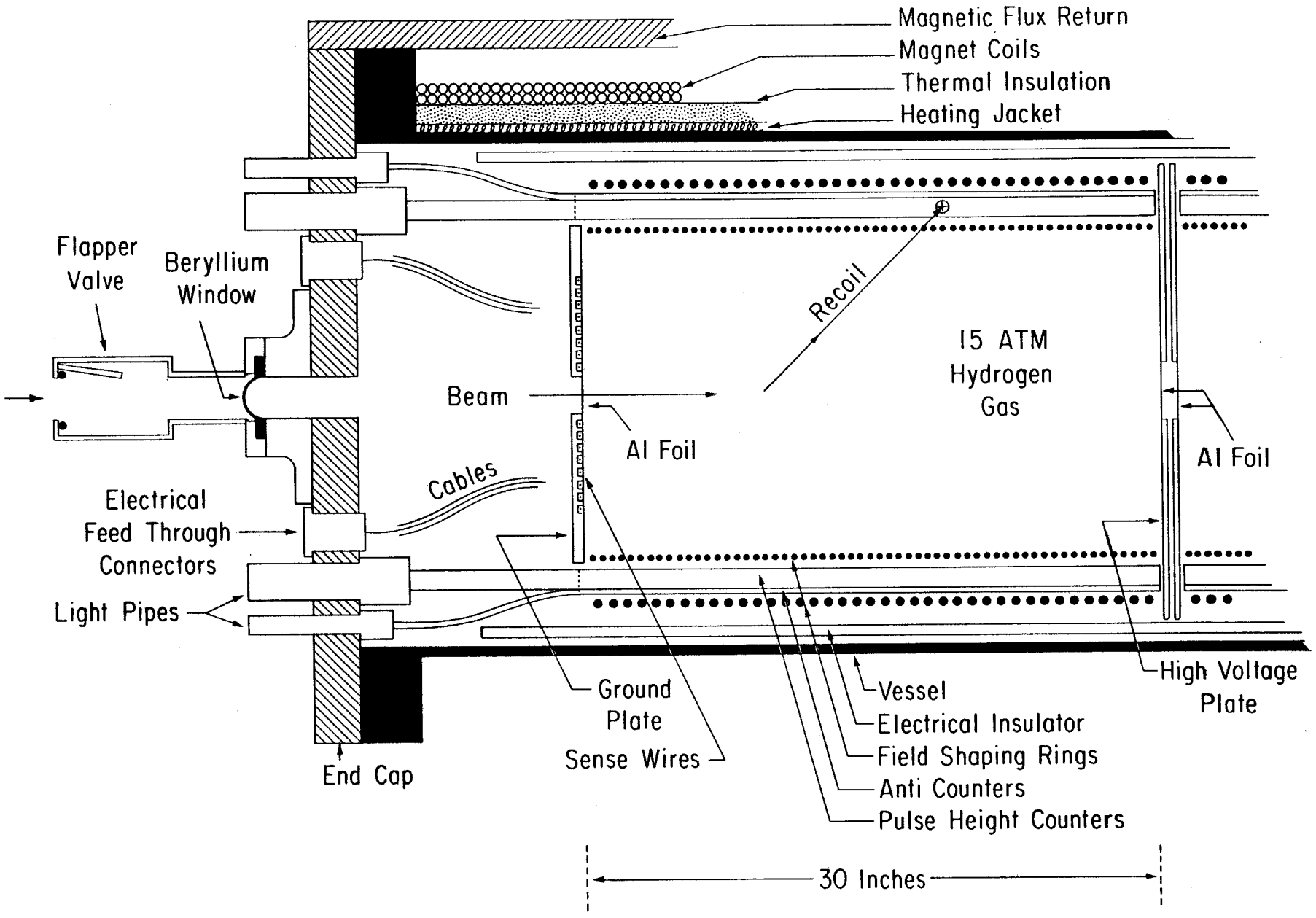
Magnetic Flux Return
Magnet Coils
Thermal Insulation
Heating Jacket
Flapper Valve
Beryllium Window
Recoil
15 ATM Hydrogen Gas
Beam
Al Foil
Al Foil
Cables
Electrical Feed Through Connectors
Light Pipes
Ground Plate
Sense Wires
End Cap
Vessel
Electrical Insulator
Field Shaping Rings
Anti Counters
Pulse Height Counters
High Voltage Plate
30 Inches

FIG. 1

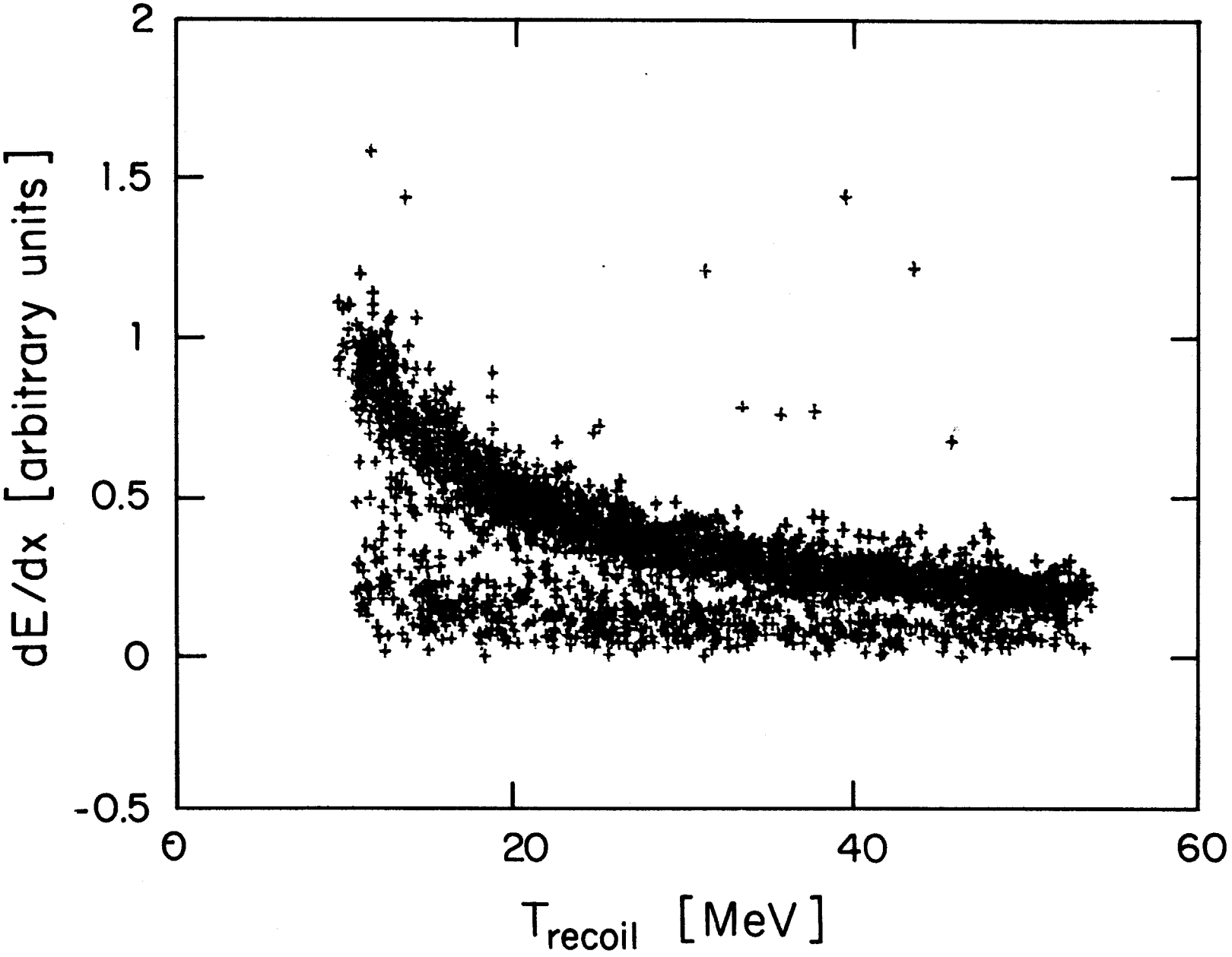

FIG. 2

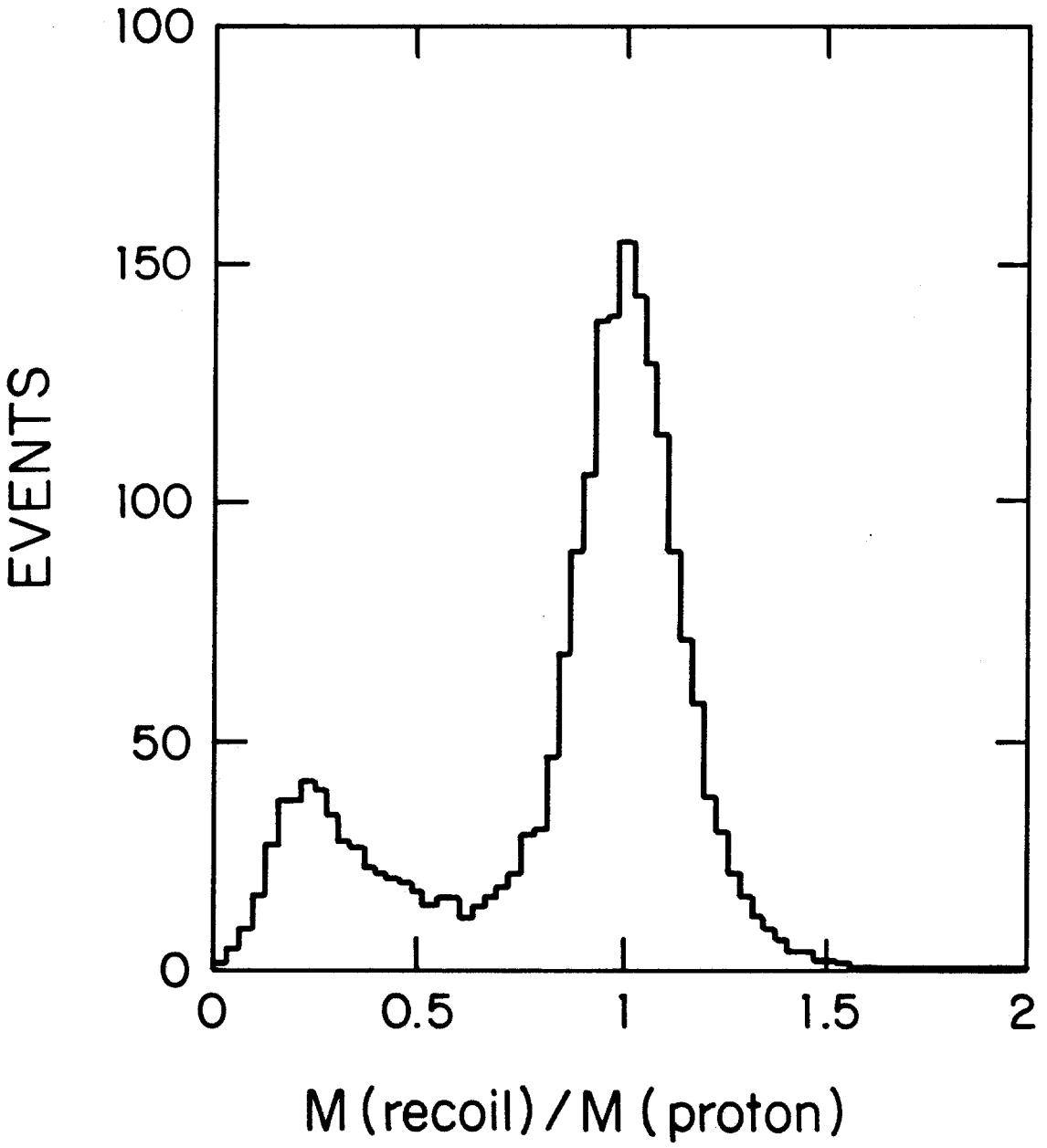

FIG. 3

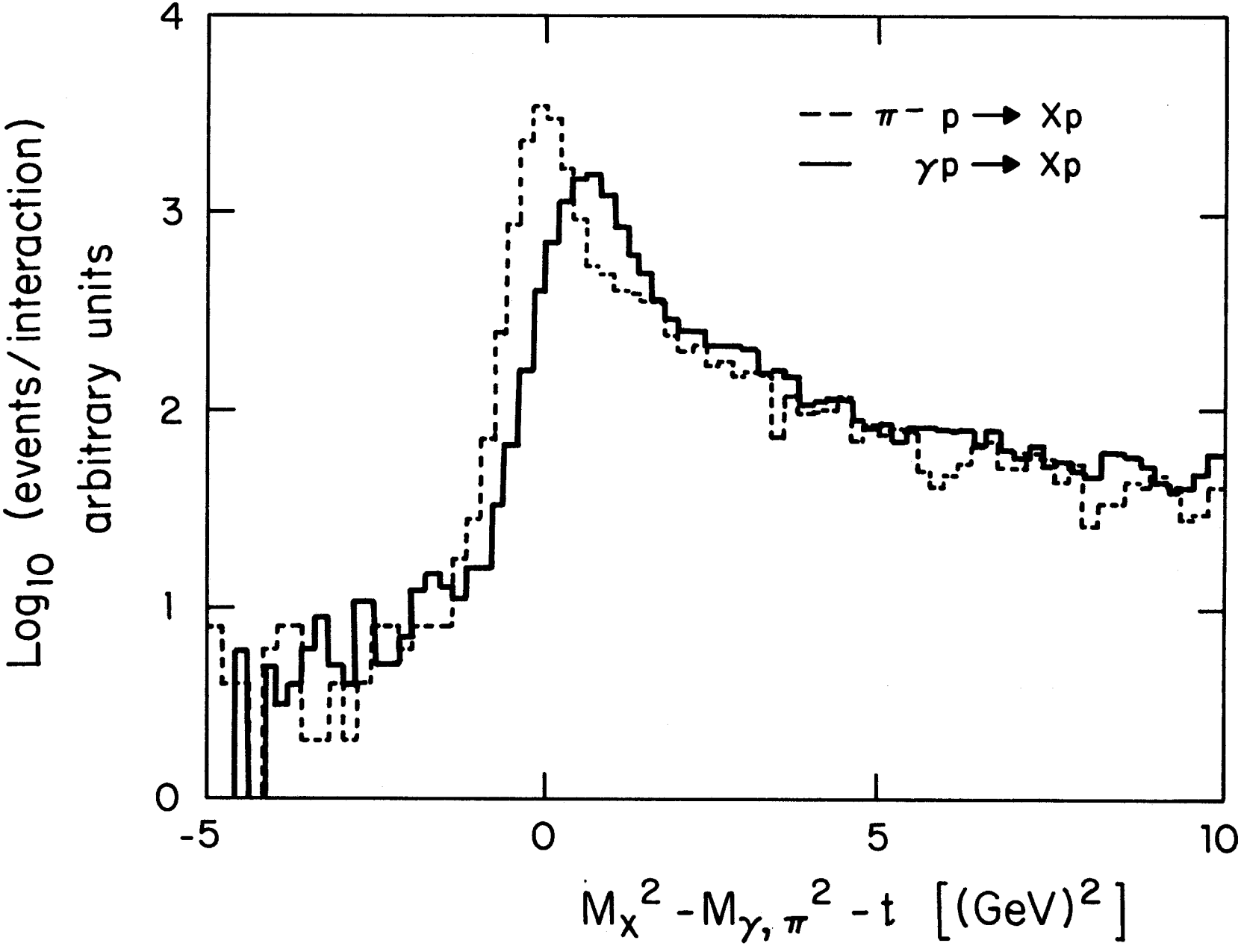
4
3
2
1
0
-5
0
5
10
$\pi^- p \rightarrow Xp$
$\gamma p \rightarrow Xp$
$\mathrm{Log_{10}}$ (events/interaction)
arbitrary units
$M_X^2 - M_{\gamma,\pi}^2 - t$ $[(\mathrm{GeV})^2]$

FIG. 4

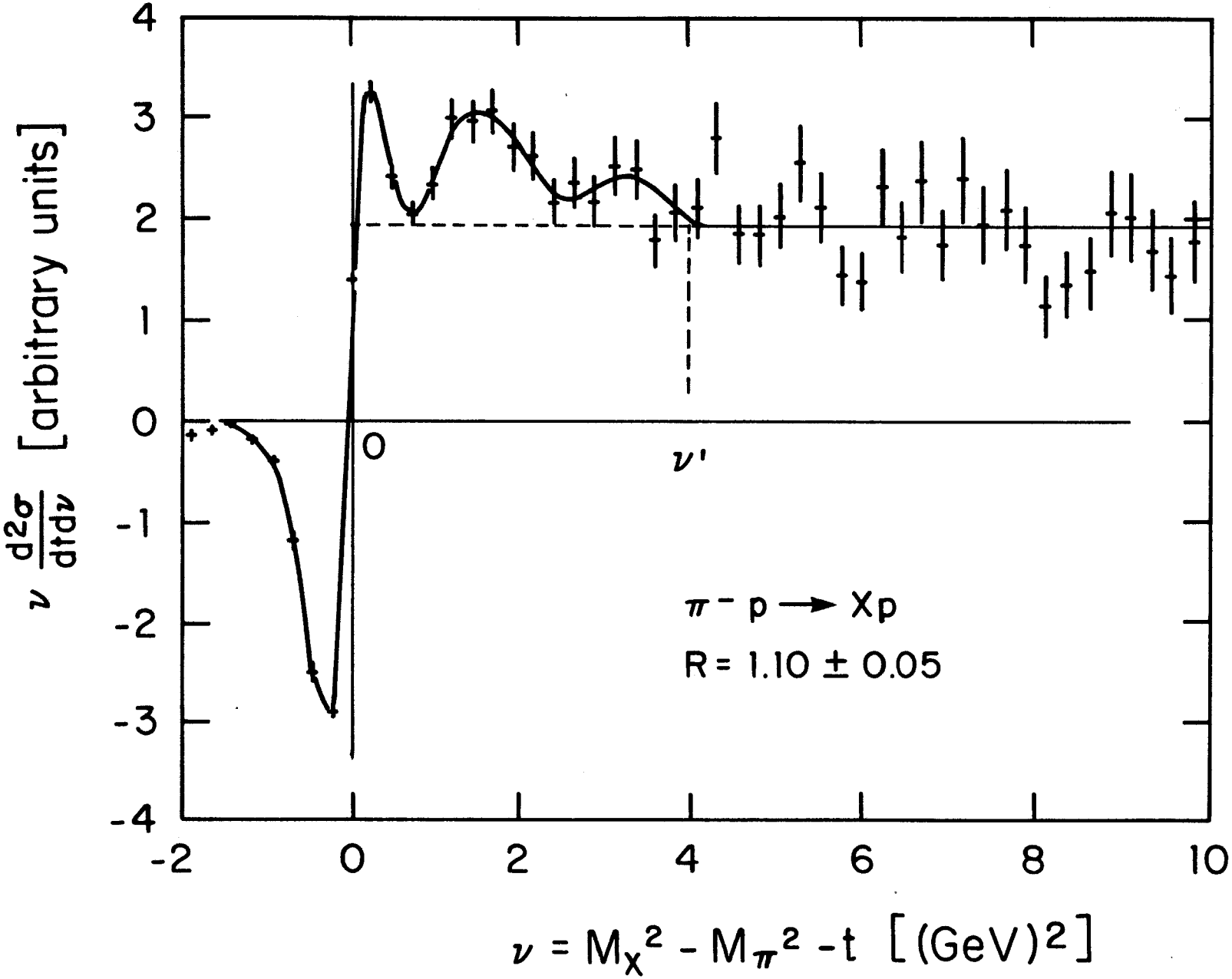
4
3
2
1
0
-1
-2
-3
-4
-2
0
2
4
6
8
10
$\nu \frac{d^2\sigma}{dtd\nu}$ [arbitrary units]
0
ν'
$\pi^- p \rightarrow Xp$
R = 1.10 ± 0.05
$\nu = M_X^2 - M_\pi^2 - t$ [(GeV)^2]

FIG. 5a

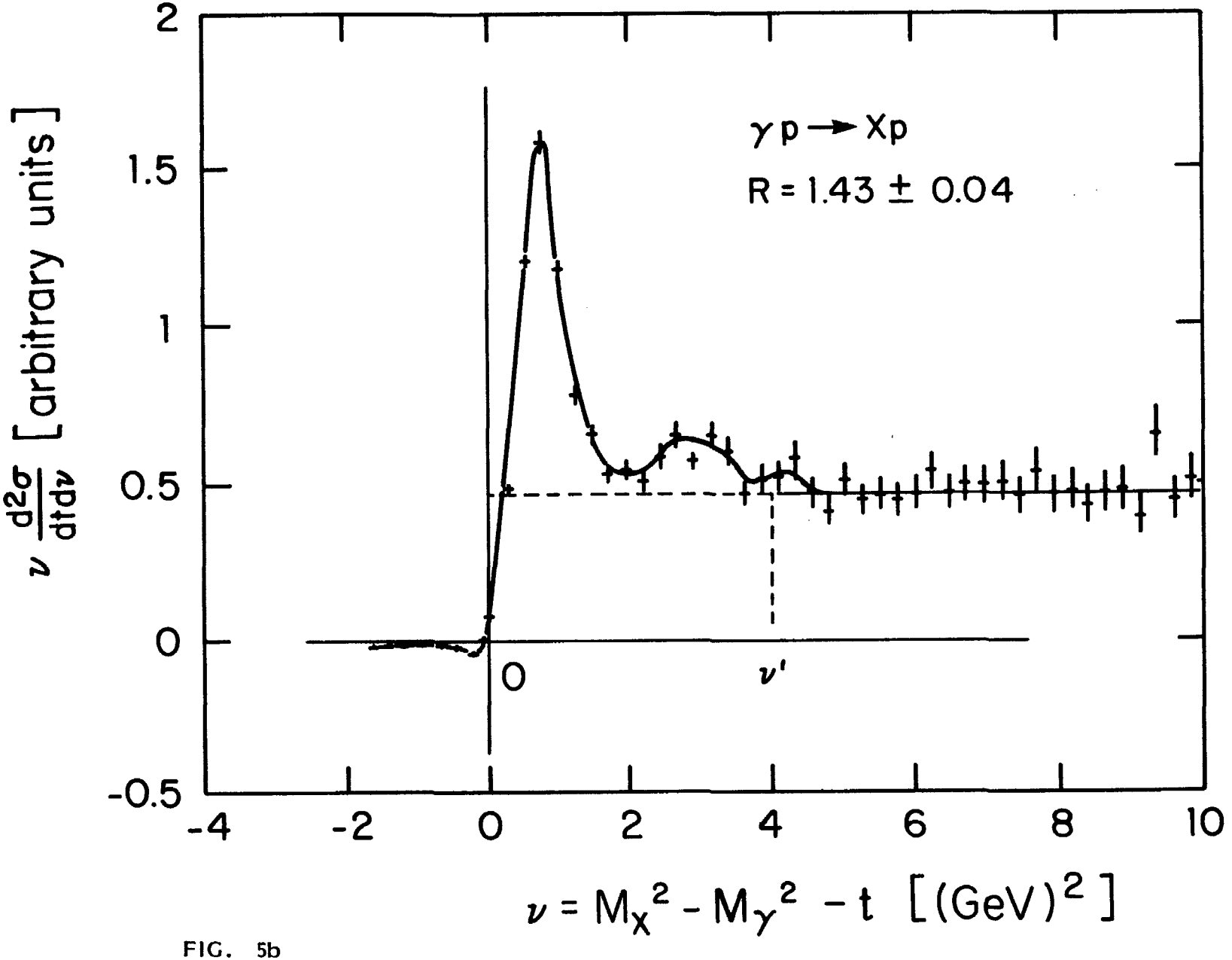
$\gamma p \rightarrow Xp$
$R = 1.43 \pm 0.04$
$\nu \frac{d^2\sigma}{dtd\nu}$ [arbitrary units]
$\nu = M_X^2 - M_\gamma^2 - t$ [(GeV)^2]
ν'
0
2
1.5
1
0.5
0
-0.5
-4
-2
0
2
4
6
8
10

FIG. 5b

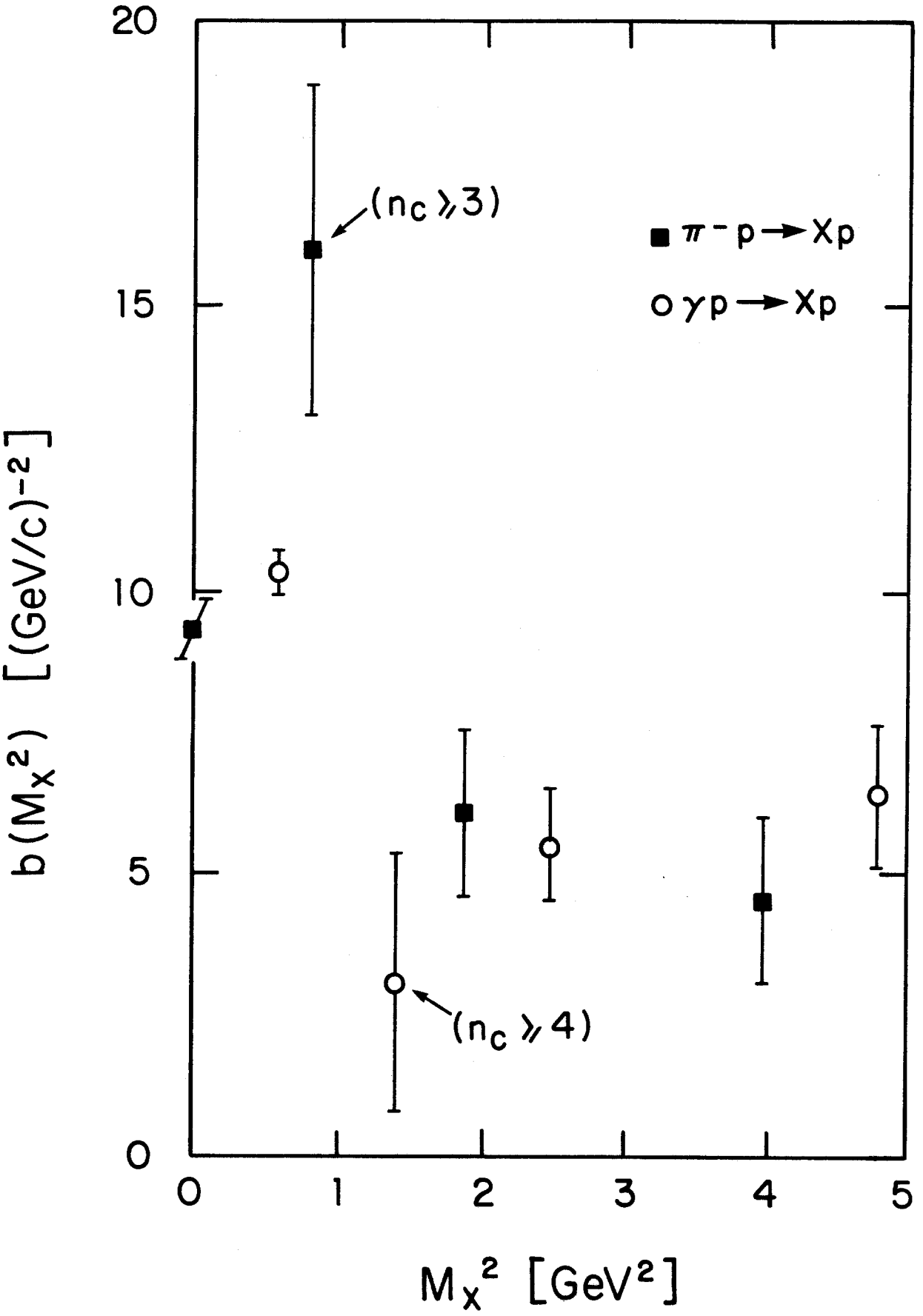
20
15
10
5
0
0
1
2
3
4
5
$b(M_X^2)$ $[(GeV/c)^{-2}]$
M_X^2 $[GeV^2]$
$(n_c \geq 3)$
$(n_c \geq 4)$
$\pi^- p \rightarrow Xp$
$\gamma p \rightarrow Xp$

FIG. 6

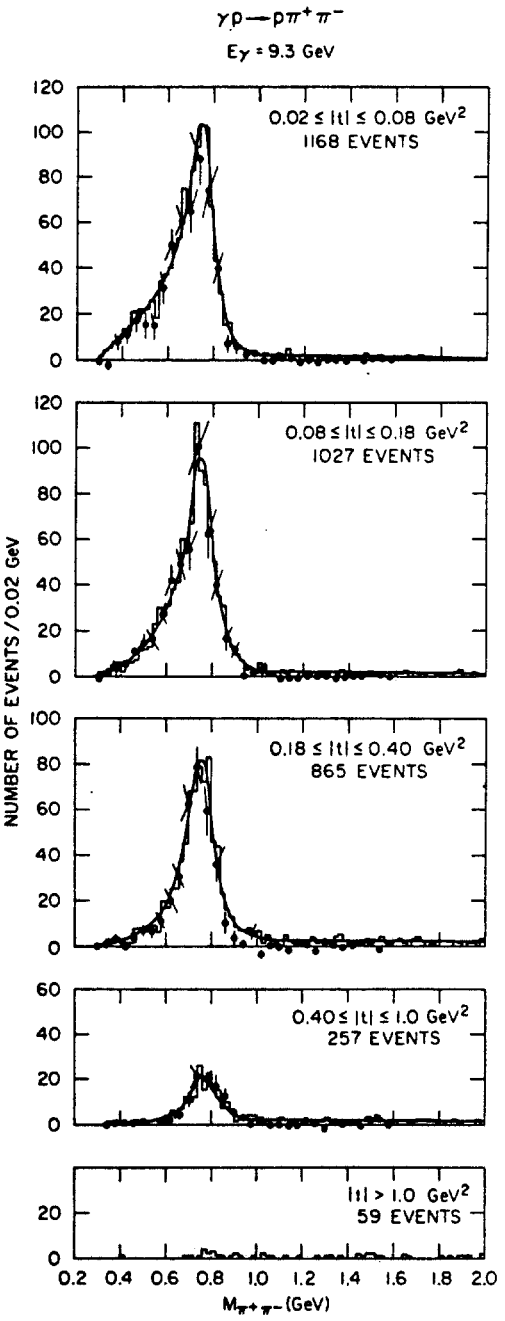

FIG. 70. Reaction $\gamma p \to p\pi^+\pi^-$ at 9.3 GeV. Distributions of the $\pi^+\pi^-$ mass for different t intervals. The helicity-conserving p-wave intensity, Π, is shown by the solid points. The curves give the result of a maximum-likelihood fit to the reaction using the Söding model (from Ballam *et al.*, 1973).

FIG. 7

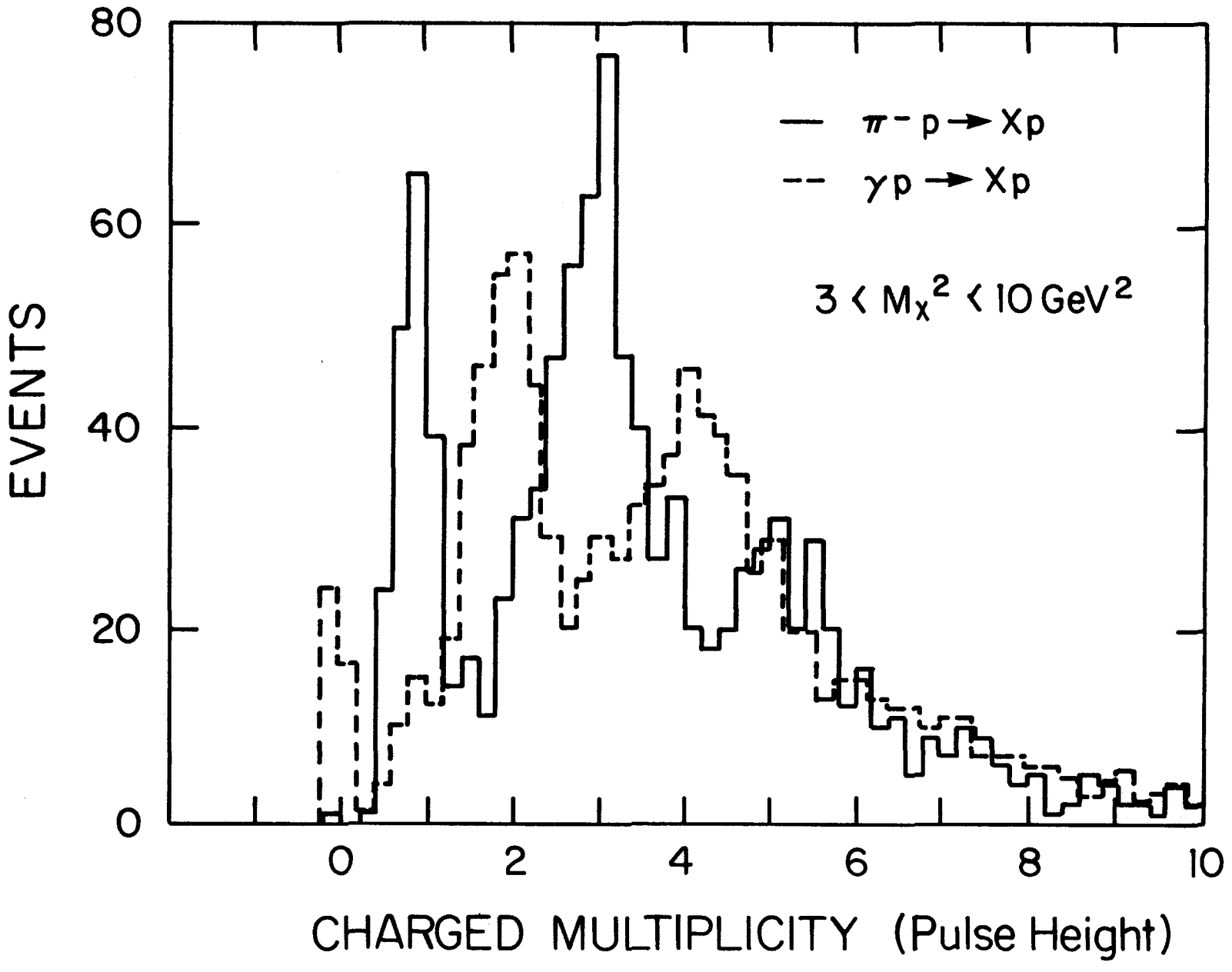
80
60
40
20
0
EVENTS
0
2
4
6
8
10
CHARGED MULTIPLICITY (Pulse Height)
π⁻p → Xp
γp → Xp
3 < M_X² < 10 GeV²

FIG. 8